

Sub-Doppler Measurements and Rotational Spectrum of $^{13}\text{C}^{18}\text{O}$

G. Klapper, F. Lewen, S. P. Belov^a, and G. Winnewisser

I. Physikalisches Institut, Universität zu Köln, Zùlpicher Str. 77, D-50937 Cologne, Germany

^a Institute of Applied Physics, Nizhnyi Novgorod 603600, Russia

Reprint requests to Prof. G. W.; Fax: 0221/470-5162; E-mail: winnewisser@ph1.uni-koeln.de

Z. Naturforsch. **55a**, 441–443 (2000); received November 29, 1999

The rotational spectrum of $^{13}\text{C}^{18}\text{O}$ has been measured up to 1 THz. The lowest rotational transitions of $^{13}\text{C}^{18}\text{O}$ ($J = 2 \leftarrow 1$ to $J = 6 \leftarrow 5$) have been measured by saturation-dip spectroscopy with an experimental accuracy of 2 kHz. These five low J rotational transitions cover the frequency range between 209 and 628 GHz. The narrow linewidths of about 20 kHz of the saturation dips allowed to resolve the two main hyperfine components. The splitting is caused by coupling of the ^{13}C nuclear spin with the rotation of the molecule. The appropriate coupling constant $C_J(^{13}\text{C}^{18}\text{O})$ is 33.90(81) kHz.

In addition we have measured in the Doppler limited mode, the line positions of the rotational transitions $J = 7 \leftarrow 6$, $J = 8 \leftarrow 7$, and $J = 9 \leftarrow 8$ with accuracies of 5 kHz. We provide a set of improved constants together with frequency predictions up to 4.1 THz ($J = 40 \leftarrow 39$).

Introduction

Astrophysically, CO is an ubiquitous molecule in the interstellar medium and plays an important role in astrophysical observations. It is used as a tracer molecule for studying planetary atmospheres and the structure of individual interstellar molecular clouds in our Galaxy. The interstellar lines of the rare isotopomers are often optically thin and are therefore more reliable tracers for column density determinations of molecular clouds. It is therefore important to provide precise laboratory transition frequencies to support astrophysical investigations.

In contrast to the main isotopomer of carbon monoxide $^{12}\text{C}^{16}\text{O}$, [1, 2], only a few publications of laboratory measurements have been reported in literature for $^{13}\text{C}^{18}\text{O}$. Sub-Doppler measurements on CO were presented in 1997 by Winnewisser et al. [2] on the main isotopomer $^{12}\text{C}^{16}\text{O}$, followed by sub-Doppler measurements on $^{13}\text{C}^{16}\text{O}$ [3].

In 1983 Guelachvili et al. [4] published Dunham coefficients of CO based on Fourier Transform measurements of $^{12}\text{C}^{16}\text{O}$, $^{12}\text{C}^{18}\text{O}$, $^{13}\text{C}^{16}\text{O}$, $^{13}\text{C}^{18}\text{O}$ of vibration-rotation spectra between 1205 and 6335 cm^{-1} . The first measurements in the submm region up to 576 GHz have been carried out on six different CO isotopomers by Winnewisser et al. [5]. The aim of the present work is to improve previous laboratory work on the isotopomer $^{13}\text{C}^{18}\text{O}$ to the level of the two more abundant isotopomers $^{12}\text{C}^{16}\text{O}$ and $^{13}\text{C}^{16}\text{O}$.

Experimental Details

Detailed descriptions of the experimental setup of the Cologne THz spectrometer can be found in [6]. Briefly, the main components consist of the stabilized radiation sources (High power backward wave oscillators (BWOs) from ISTOK, Russia; reference synthesizer KVARZ, Russia), the absorption cell, and the InSb hot electron bolometer (QMC, UK). The BWOs used for these measurements operate in the frequency range from 200 to 1000 GHz. The BWO radiation is carefully focused through a 3.5 m absorption cell with a diameter of 10 cm. The windows of the cell and the lenses are made of high density polyethylene (HDPE), which offers a lower absorption coefficient than PTFE [7]. In the case of the sub-Doppler measurements, the sample pressure in the absorption cell was maintained near 3 μbar . We used a 99% enriched ^{13}C sample. The ^{18}O content was not specified, but it may also have been slightly enriched due to the ^{13}C enrichment process.

Results

In Table 1 the frequencies of the newly measured transitions of $^{13}\text{C}^{18}\text{O}$ are summarized together with the transition frequency of the $J = 1 \leftarrow 0$ line measured by Winnewisser et al. [6]. The line center frequencies were derived from the measured data points by fitting them to a parabolic function. The present Lamb dip measurements are reliable to about 2 kHz. The Doppler-limited measurements can be trusted to 5 kHz.

0932-0784 / 00 / 0300-0441 \$ 06.00 © Verlag der Zeitschrift für Naturforschung, Tübingen · www.znaturforsch.com



Dieses Werk wurde im Jahr 2013 vom Verlag Zeitschrift für Naturforschung in Zusammenarbeit mit der Max-Planck-Gesellschaft zur Förderung der Wissenschaften e.V. digitalisiert und unter folgender Lizenz veröffentlicht: Creative Commons Namensnennung-Keine Bearbeitung 3.0 Deutschland Lizenz.

Zum 01.01.2015 ist eine Anpassung der Lizenzbedingungen (Entfall der Creative Commons Lizenzbedingung „Keine Bearbeitung“) beabsichtigt, um eine Nachnutzung auch im Rahmen zukünftiger wissenschaftlicher Nutzungsformen zu ermöglichen.

This work has been digitalized and published in 2013 by Verlag Zeitschrift für Naturforschung in cooperation with the Max Planck Society for the Advancement of Science under a Creative Commons Attribution-NoDerivs 3.0 Germany License.

On 01.01.2015 it is planned to change the License Conditions (the removal of the Creative Commons License condition “no derivative works”). This is to allow reuse in the area of future scientific usage.

Table 1. Sub-Doppler and doppler resolved rotational transitions of $^{13}\text{C}^{18}\text{O}$.

| J' | F' | \leftarrow | J'' | F'' | Obs. Frequencies ^a [MHz] | O–C [kHz] | Rel. Int. |
|------|------|--------------|-------|-------|--|--------------|-----------|
| 1 | | \leftarrow | 0 | | 104 711.4035 (57) ^b | 8.1 | |
| 2 | 1.5 | \leftarrow | 1 | 0.5 | 209 419.1380 (20) | –3.7 | 0.333 |
| 2 | 2.5 | \leftarrow | 1 | 1.5 | 209 419.1721 (20) | –3.5 | 0.600 |
| 3 | 2.5 | \leftarrow | 2 | 1.5 | 314 119.6453 (20) | 4.8 | 0.400 |
| 3 | 3.5 | \leftarrow | 2 | 2.5 | 314 119.6752 (20) | 0.8 | 0.571 |
| 4 | 3.5 | \leftarrow | 3 | 2.5 | 418 809.2422 (20) | –0.5 | 0.429 |
| 4 | 4.5 | \leftarrow | 3 | 3.5 | 418 809.2763 (20) | –0.3 | 0.556 |
| 5 | 4.5 | \leftarrow | 4 | 3.5 | 523 484.3138 (20) | –2.4 | 0.444 |
| 5 | 5.5 | \leftarrow | 4 | 4.5 | 523 484.3486 (20) | –1.5 | 0.546 |
| 6 | 5.5 | \leftarrow | 5 | 4.5 | 628 141.2299 (20) | 1.3 | 0.455 |
| 6 | 6.5 | \leftarrow | 5 | 5.5 | 628 141.2665 (20) | 4.0 | 0.539 |
| 7 | | \leftarrow | 6 | | 732 776.360 (5) | –4.9 | |
| 8 | | \leftarrow | 7 | | 837 386.054 (5) | –4.8 | |
| 9 | | \leftarrow | 8 | | 941 966.695 (5) | –0.2 | |

^a For unresolved hfs the F values and relative intensities are omitted. In these cases the calculated frequencies were obtained by using weighted averages of individual hfs components. The errors are 1σ .

^b Observed frequency taken from Winnewisser *et al.* [5].

Table 2. Molecular constants of $^{13}\text{C}^{18}\text{O}$.

| Constant | This work | MMW data ^a | Unit |
|----------|-------------------|-----------------------|------|
| B_0 | 52 355.99739 (11) | 52 356.0022 (7) | MHz |
| D_0 | 151.3415 (27) | 151.416 (18) | kHz |
| H_0 | – | 0.1231 ^b | Hz |
| C_I | 33.90 (81) | – | kHz |

^a Winnewisser *et al.* [5].

^b Values derived from Guelachvili *et al.* [4].

Table 3. Predicted frequencies of rotational transitions of $^{13}\text{C}^{18}\text{O}$.

| J' | F' | \leftarrow | J'' | F'' | Calc. Frequencies ^a [MHz] |
|------|------|--------------|-------|-------|---|
| 1 | | \leftarrow | 0 | | 104 711.39541 (38) |
| 2 | | \leftarrow | 1 | | 209 419.15863 (71) |
| 3 | | \leftarrow | 2 | | 314 119.65745 (93) |
| 4 | | \leftarrow | 3 | | 418 809.2597 (10) |
| 5 | | \leftarrow | 4 | | 523 484.3331 (11) |
| 6 | | \leftarrow | 5 | | 628 141.2456 (12) |
| 7 | | \leftarrow | 6 | | 732 776.3649 (19) |
| 8 | | \leftarrow | 7 | | 837 386.0588 (32) |
| 9 | | \leftarrow | 8 | | 941 966.6952 (51) |
| 10 | | \leftarrow | 9 | | 1 046 514.6418 (76) |
| 11 | | \leftarrow | 10 | | 1 151 026.266 (11) |
| 12 | | \leftarrow | 11 | | 1 255 497.937 (15) |
| 13 | | \leftarrow | 12 | | 1 359 926.021 (19) |
| 14 | | \leftarrow | 13 | | 1 464 306.887 (25) |
| 15 | | \leftarrow | 14 | | 1 568 636.901 (31) |
| 16 | | \leftarrow | 15 | | 1 672 912.433 (39) |
| 17 | | \leftarrow | 16 | | 1 777 129.850 (47) |
| 18 | | \leftarrow | 17 | | 1 881 285.519 (57) |
| 19 | | \leftarrow | 18 | | 1 985 375.809 (68) |
| 20 | | \leftarrow | 19 | | 2 089 397.087 (79) |
| 21 | | \leftarrow | 20 | | 2 193 345.722 (93) |
| 22 | | \leftarrow | 21 | | 2 297 218.08 (11) |
| 23 | | \leftarrow | 22 | | 2 401 010.53 (12) |
| 24 | | \leftarrow | 23 | | 2 504 719.44 (14) |
| 25 | | \leftarrow | 24 | | 2 608 341.18 (16) |
| 26 | | \leftarrow | 25 | | 2 711 872.11 (18) |
| 27 | | \leftarrow | 26 | | 2 815 308.60 (20) |
| 28 | | \leftarrow | 27 | | 2 918 647.03 (23) |
| 29 | | \leftarrow | 28 | | 3 021 883.75 (25) |
| 30 | | \leftarrow | 29 | | 3 125 015.14 (28) |
| 31 | | \leftarrow | 30 | | 3 228 037.57 (31) |
| 32 | | \leftarrow | 31 | | 3 330 947.39 (34) |
| 33 | | \leftarrow | 32 | | 3 433 740.99 (38) |
| 34 | | \leftarrow | 33 | | 3 536 414.72 (41) |
| 35 | | \leftarrow | 34 | | 3 638 964.96 (45) |
| 36 | | \leftarrow | 35 | | 3 741 388.07 (49) |
| 37 | | \leftarrow | 36 | | 3 843 680.42 (53) |
| 38 | | \leftarrow | 37 | | 3 945 838.39 (58) |
| 39 | | \leftarrow | 38 | | 4 047 858.32 (63) |
| 40 | | \leftarrow | 39 | | 4 149 736.61 (68) |

^a For frequencies the hfs and relative intensity is omitted.

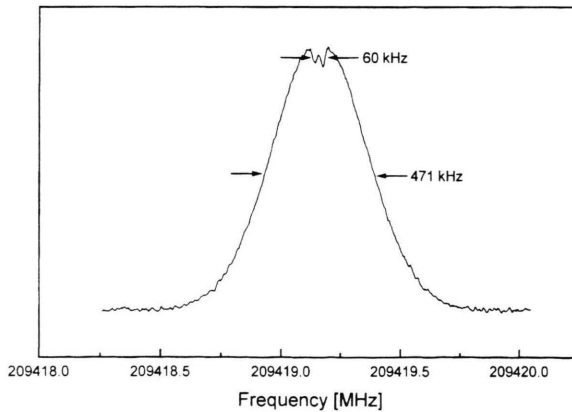
Lamb Dip Spectrum ($J=2 \leftarrow 1$)

Fig. 1. The Lamb-dip spectrum of the $J=2 \leftarrow 1$ transition of $^{13}\text{C}^{18}\text{O}$ at 209 GHz superimposed on the Doppler profile.

The achievable accuracy for unblended, fully resolved Lamb dip measurements in the sub-millimeter wave region recorded with a good signal to noise ratio is estimated to be around 500 Hz [2]. However, the present accuracies are estimated to be about 2 kHz, i.e. somewhat lower than the achievable 500 Hz. The reason is twofold: (i) the components of the hyperfine structure are slightly overlapping and (ii) the signal-to-noise ratio of the $^{13}\text{C}^{18}\text{O}$ measurements is limited. In a series of figures we present some of the recorded Lamb dip spectra. Figure 1 presents the Lamb dips of the two hyperfine components superimposed on the Doppler line profile of the $J=2 \leftarrow 1$ transition. The linewidth of the Doppler profile is about

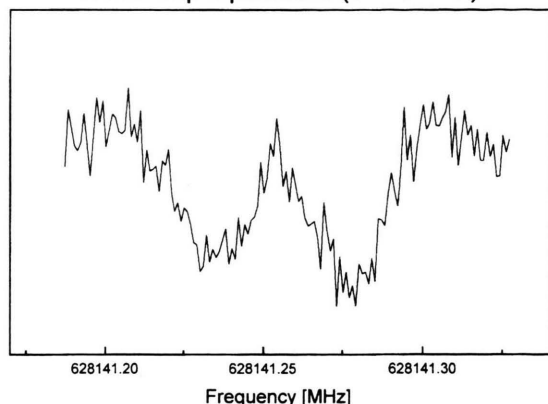
Lamb Dip Spectrum ($J = 6 \leftarrow 5$)

Fig. 2. The highest J rotational transition of $^{13}\text{C}^{18}\text{O}$ measured in sub-Doppler resolution.

471 kHz whereas the linewidths of the hyperfine components are about 21 kHz, just allowing to resolve the two main hyperfine components. The hyperfine components are separated by 34 kHz. The third hf-component was too weak for detection.

The $J = 6 \leftarrow 5$ transition of 628 GHz (Fig. 2), where the two strongest hyperfine components have a separation of only 36.6 kHz, is recorded with similar accuracy.

This is the highest frequency Lamb dip spectrum obtained in this study.

The 13 newly measured rotational transitions (Table 1) of $^{13}\text{C}^{18}\text{O}$ were subjected to a least squares fit, in which each line was weighted proportionally to the inverse square of its assigned experimental uncertainty. For unresolved hyperfine splittings, the calculated frequencies were determined in the fit by using intensity-weighted averages of the individual hyperfine-components. The σ of the fit is 4 kHz. In Table 2 we give a summary of the newly determined two constants B_0 and D_0 together with the nuclear spin-rotation constant $C_I(^{13}\text{C}^{18}\text{O})$. The ratio $C_I(^{13}\text{C})/B_0(^{13}\text{C})$ of the isotopomers $^{13}\text{C}^{18}\text{O}$ and $^{13}\text{C}^{16}\text{O}$ [3] agrees within less than 1 σ and is therefore an excellent measure of the internal consistency of the data. Table 3 lists the frequency predictions up to 4.1 THz based on our newly determined constants.

Acknowledgements

This work has been supported in part by the Deutsche Forschungsgemeinschaft (DFG) via Grant SFB 301 and the special funding from the Science Ministry of the state Nordrhein-Westfalen. The work of S.P.B. at Cologne was made possible by the DFG through grants aimed to support Eastern and Central European Countries and the republics of the former Soviet Union.

- [1] O. Varberg and K. Evenson, *Astrophys. J.* **385**, 763 (1992).
- [2] G. Winnewisser, S. P. Belov, Th. Klaus, and R. Schieder, *J. Mol. Spectrosc.* **184**, 468 (1997).
- [3] G. Klapper, F. Lewen, R. Gendriesch, S. P. Belov, and G. Winnewisser, *J. Mol. Spectrosc.* (1999, in press).
- [4] G. Guelachvili, G. De Villeneuve, R. Farrenq, W. Urban, and J. Verges, *J. Mol. Spectrosc.* **98**, 64 (1983).
- [5] M. Winnewisser, B. P. Winnewisser, and G. Winnewisser, in *Molecular Astrophysics, Series C*, Vol. 157, pp. 375–402, Reidel, Dordrecht 1985.
- [6] G. Winnewisser, *Vibr. Spectrosc.* **8**, 241 (1995).
- [7] C. Winnewisser, F. Lewen, and H. Helm, *Appl. Phys. A* **66**, 593 (1998).